European Journal of Immunology

TLR9 activation is a key event for the maintenance of a mycobacterial antigen-elicited pulmonary granulomatous response

Toshihiro Ito[1,2], Matthew Schaller[1], Cory M. Hogaboam[1], Theodore J. Standiford[3], Stephen W. Chensue[1,4] and Steven L. Kunkel[1]

[1] Department of Pathology, University of Michigan Medical School, Ann Arbor, MI, USA
[2] Second Department of Internal Medicine, Nara Medical University, Nara, Japan
[3] Division of Pulmonary and Critical Care Medicine, Department of Medicine, University of Michigan Medical Center, Ann Arbor, MI, USA
[4] Department of Pathology and Laboratory Medicine, Veterans Affairs Ann Arbor Healthcare System, Ann Arbor, MI, USA

Received 22/6/07
Revised 12/7/07
Accepted 13/8/07

[DOI 10.1002/eji.200737603]

Type 1 (Th1) granulomas can be studied in mice sensitized with mycobacterium antigens followed by challenge of agarose beads covalently coupled to purified protein derivative. TLR9 is known to play a role in the regulation of Th1 responses; thus, we investigated the role of TLR9 in granuloma formation during challenge with mycobacterium antigens and demonstrated that mice deficient in TLR9 had increased granuloma formation, but a dramatically altered cytokine phenotype. Th1 cytokine levels of IFN-γ and IL-12 in the lungs were decreased in TLR9$^{-/-}$ mice when compared to wild-type mice. In contrast, Th2 cytokine levels of IL-4, IL-5, and IL-13 were increased in TLR9$^{-/-}$ mice. The migration of CD4^{+} T cells in the granuloma was impaired, while the number of F4/80^{+} macrophages was increased in TLR9$^{-/-}$ mice. Macrophages in the lungs of the TLR9-deficient animals with developing granulomas expressed significantly lower levels of the classically activated macrophage marker, nitric oxide synthase, but higher levels of the alternatively activated macrophage markers such as 'found in inflammatory zone-1′ antigen and Arginase-1. These results suggest that TLR9 plays an important role in maintaining the appropriate phenotype in a Th1 granulomatous response.

Key words: Granuloma · Innate immunity · Macrophages · Th1/Th2 · TLR

Introduction

The lung is one of the most immunologically challenged organs and can be affected by a number of granuloma-inducing agents including non-infectious environmental factors and infectious mycobacteria, fungi, and parasites [1, 2]. Among these, tuberculosis, a lung disease caused by *Mycobacterium tuberculosis*, remains a significant cause of morbidity and mortality throughout the world [3]. A granuloma, composed of a group of epithelioid macrophages surrounded by a lymphocyte cuff, is a characteristic pathophysiological feature induced by mycobacterial infections and is an important element of the host defense system [2, 4]. Interestingly, little is known about the immunological and pathological mechanisms that control granuloma formation in the lung. We previously described a model of polarized Th1 cell-mediated anamnestic pulmonary granulomatous inflammation in sensitized mice induced by pulmonary embolization of agarose beads coated with covalently

Correspondence: Steven L. Kunkel, Immunology Program, Department of Pathology, University of Michigan Medical School, 4701 BSRB, 109 Zina Pitcher Place, Ann Arbor, MI 48109–2200, USA
Fax: +1-734-764-2397
e-mail: slkunkel@umich.edu

Abbreviations: **FIZZ-1:** found in inflammatory zone-1 · **IP-10:** IFN-γ-inducible protein 10 · **M1:** classically activated · **M2:** alternatively activated · **PPD:** purified protein derivative

bound antigens of *Mycobacteria bovis* purified protein derivative (PPD) [5–9]. Cytokine and chemokine analyses of this model indicated protein profiles consistent with a predominant Th1 cell involvement and histologically showed an enrichment of macrophages at the granuloma sites [10, 11].

Macrophages become activated and express distinct patterns of chemokine and cytokines in response to exogenous signals such as pathogen byproducts and soluble immune mediators. They can be activated by either a classical (M1) or alternative (M2) pathway depending on the stimulus [12, 13]. M1 macrophages, induced by proinflammatory molecules such as IFN-γ and LPS, play an important role in the elimination of various pathogens [14]. They up-regulate the expression of proinflammatory cytokines (TNF-α, IL-12) and are able to secrete nitric oxide (NO), a free radical that is toxic to bacteria and other pathogens, *via* activation of inducible NO synthase (iNOS) [15]. M2 macrophages are activated in response to the Th2 cytokines, IL-4 and IL-13 [16], and are functionally and biochemically distinct from M1 macrophages [17]. They produce low levels of proinflammatory cytokines, and fail to produce NO [17]. Instead, arginase production and induction of FIZZ-1 (found in inflammatory zone-1) are increased [18, 19]. It has been demonstrated that M2 macrophages are generated during the development of Th2 granulomas, for example those elicited by *Schistosoma mansoni* eggs, and the M2 macrophages down-modulated Th1 responses [20]. However, the precise mechanisms that regulate M1 and M2 activation within the context of granuloma formation remain to be determined.

Macrophages respond to microbial ligands through TLR [21], which are key molecules in the recognition of microbial components during infection and are known to play an important role in both the innate and adaptive immune response [22–24]. Microbial products, including mycobacterium antigen, activate specific TLR, which in turn induce specific gene transcription resulting in the up-regulation and secretion of select chemokines and cytokines [25–27]. When activated, TLR specifically recruit adapter proteins (MyD88, MAL, TRIF, TRAM, and SARM), which are essential for the TLR gene transcription signaling cascade [28, 29]. Recent studies have provided new insights on how TLR are involved in the recognition of specific pathogens, and have clarified their roles in both the innate and adaptive immune response. For example, mycobacterial components act as agonists for TLR, and mice that are deficient in the TLR adaptor molecule, MyD88, show an impaired response to mycobacterial antigens, which is correlated with decreased NOS2 expression and decreased IFN-γ production [30]. Although the response to mycobacterium antigens appears dependent on MyD88 [30, 31], the TLR involved has not been identified. All TLR, except TLR3, have at least one signaling pathway dependent on MyD88 [22]. The involvement of different TLR, for example, TLR2, TLR4, and TLR6, in the recognition of mycobacterium antigens has been shown in mice and humans [25, 32–37]. TLR9 recognizes as ligands viral and bacterial CpG-DNA motifs, which when bound to TLR9 on macrophages and DC, causes their activation [38–40]. A number of studies indicate that CpG-DNA TLR9 interaction can drive a Th1 immune response, as evidenced by a Th1-dominated cytokine profile [41–43]. A recent report demonstrated that TLR9 played an important role in the regulation of the mycobacteria-induced Th1 responses during *M. tuberculosis* infection *in vivo* [44]. Although these studies showed the importance of TLR9 in driving the Th1 response to microbial infection, none investigated the role of TLR9 in pulmonary granuloma formation during mycobacterium antigen challenge.

In the present study, Th1 cytokines and chemokine [IFN-γ, IL-12, and IFN-γ-inducible protein 10, (IP-10)] and Th2 cytokines (IL-4, IL-5, and IL-13) profiles were determined in both WT and TLR9$^{-/-}$ mice using a PPD bead-induced experimental lung granuloma model. We demonstrate that TLR9-deficient mice developed a type-2-like response with significantly larger granulomas and increased accumulation of eosinophils compared to control mice granulomas. This greater granulomatous and enhanced eosinophilic response was associated with a selectively abrogated type-1 and enhanced type-2 cytokine profile in the lung. We also found that the recruitment of CD4$^+$ T cells to granulomas was impaired, while increased numbers of F4/80$^+$ macrophages were observed. Our results further showed that lung macrophages were shifted from classically activated (M1) to alternatively activated (M2) in TLR9$^{-/-}$ mice. Taken together, our data support the premise that TLR9 plays a key role in the induction of a Th1 cell-mediated hypersensitive granuloma formation.

Results

Effect on TLR9 gene knockout on pulmonary granuloma size and composition

To investigate the role of TLR9 on the effector stage of antigen-bead elicited responses, mice were sensitized i.p. with 0.5 mL CFA and 14 days later were challenged *via* a tail vein with PPD-coupled beads. The beads embolize to the lungs where they elicit a synchronous granulomatous inflammatory response that spreads into the interstitium and is histologically similar to those observed in live mycobacterium infections. We characterized the histology of antigen bead-challenged lungs throughout an 8-day period following injection of the

beads. The antigen-induced response in the TLR9$^{-/-}$ mice showed significantly larger granulomas compared with WT mice on day 2 (Fig. 1A and B), day 4 (Fig. 1C and D), and day 8 (Fig. 1E and F). The size was the largest on day 4 in both WT and TLR9$^{-/-}$ mice, and the differences between these mice were significant on day 2 (5800.4 ± 1510.7 μm^2 *vs*. 8376.2 ± 1736.5 μm^2), day 4 (8086.7 ± 1811.6 μm^2 *vs*. 13061.6 ± 3016.6 μm^2) and day 8 (5442.2 ± 1375.6 μm^2 *vs*. 8549.1 ± 1957.8 μm^2) (WT *vs*. TLR9$^{-/-}$ mice, respectively) (Fig. 2). Histologically, TLR9$^{-/-}$ mice displayed increased eosinophils in lung granulomas compared with WT mice at day 8 (Fig. 3A). Upon quantification, eosinophils in lung granulomas were significantly higher in TLR9$^{-/-}$ (0.589 ± 0.232/100 μm^2) compared with in WT mice (0.099 ± 0.062/100 μm^2) (Fig. 3B).

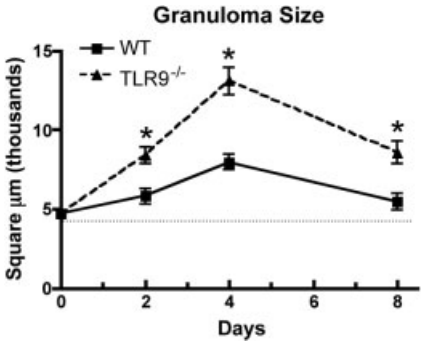

Figure 2. Time course of innate granulomatous inflammation in response to PPD-coated agarose beads during an 8-day study period. Points are mean granuloma cross-sectional area (μm^2) ± SEM with five mice per point and with 20 granulomas measured per lung. The dotted line indicates average size of bead only. *$p<0.001$ compared with granuloma size measure in WT mice.

Alternation in the cytokine and chemokine profile in whole lungs from TLR9$^{-/-}$ mice

To help elucidate the mechanism underlying the changes in pulmonary granuloma size and cellular content in TLR9$^{-/-}$ *versus* WT mice, we profiled cytokine and chemokine expression in lungs. In the present study, whole lungs from TLR9$^{-/-}$ mice had significantly lower levels of both mRNA and protein of IFN-γ and IP-10, in comparison with WT mice (Fig. 4A–D). Moreover, the cytokine profile in the whole-lung samples revealed a significant decrease in IL-12p70 protein level in TLR9$^{-/-}$ mice at days 2 and 4 after PPD bead challenge (Fig. 4F). IL-12 is a heterodimeric cytokine, consisting of covalently bound p40 and p35 subunits, and TLR9$^{-/-}$ mice showed lower mRNA levels for both of these subunits

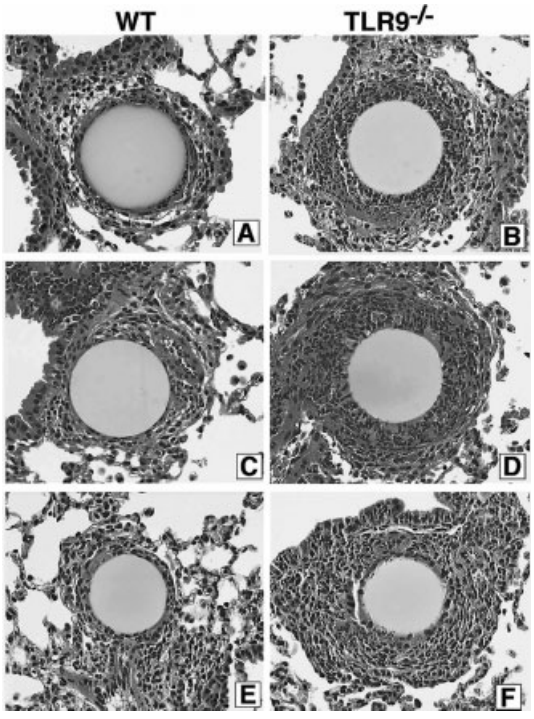

Figure 1. Histological appearance of pulmonary granulomas induced by PPD beads. Lung tissue from WT (A, C, and E) and TLR9$^{-/-}$ mice (B, D, and F) was analyzed 2, 4, and 8 days after i.v. injection with 5500 PPD beads. H&E-stained lung sections from WT or TLR9$^{-/-}$ mice are shown (magnification, ×400); n=5 animals/time point/group.

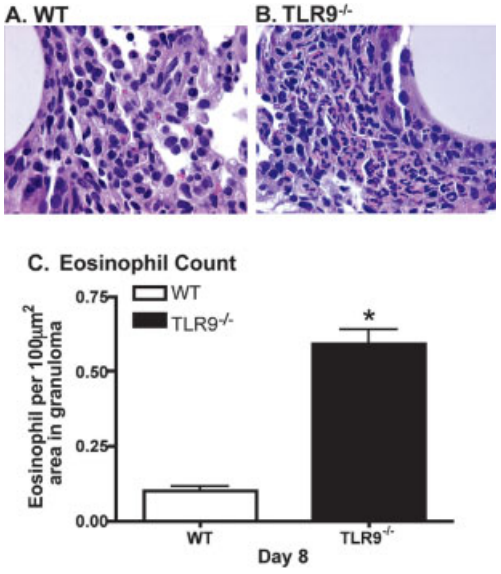

Figure 3. Increased number of eosinophils in TLR9$^{-/-}$ mice during granuloma formation. Lung tissue from WT (A) and TLR9$^{-/-}$ (B) mice was analyzed at 8 days after PPD-bead challenge. High-power micrographs of lung sections of TLR9$^{-/-}$ mice display aggregation of eosinophils around PPD bead (magnification, ×1000). No eosinophils were detected 2 or 4 days post injection. (C) Quantification of eosinophil numbers in pulmonary granulomas. Granulomas, 20 per mouse, were analyzed for the eosinophil infiltrate. Results are expressed as mean ± SEM per 100 μm^2 area in granuloma from five mice/group using computerized morphometry. *$p<0.001$ *versus* WT.

compared to WT mice (Fig. 4E and G). While TLR9$^{-/-}$ mice showed a defect in Th1 cytokine and chemokine production in response to PPD beads, mRNA and protein levels of cytokines that promote the Th-2 biased immune response (*i.e.*, IL-4, IL-5 and IL-13), were significantly increased in TLR9$^{-/-}$ mice (Fig. 5A, C, and E). ELISA analysis confirmed that the protein level of IL-4 and IL-5 was increased at 8 days after bead challenge (Fig. 5B and D), and that IL-13 was higher throughout the 8-day period in TLR9$^{-/-}$ mice (Fig. 5F).

Decreased recruitment of CD4$^+$ T cells in TLR9$^{-/-}$ mice

Flow cytometric analysis revealed that the number of CD3$^+$CD4$^+$ T cells was severely decreased (Fig. 6A), while the number of F4/80$^+$ macrophages was increased in TLR9-deficient lungs at 4 days after PPD-bead challenge (Fig. 6B). These results were also supported by immunohistochemical analysis. (Fig. 6C and D), which shows more F4/80$^+$ staining cells and a decrease in CD4$^+$ cells associated with the local lung granuloma.

TLR9$^{-/-}$ mice demonstrated a M2 macrophage phenotype during pulmonary granuloma formation

Because the number of macrophages in the pulmonary granulomas was increased in TLR9$^{-/-}$ mice, we assessed the phenotype of the granuloma evolving in WT and TLR9$^{-/-}$ mice for macrophage markers characteristic of either an M1 or M2 response. The mRNA expression level of iNOS, which is a macrophage marker for an M1 phenotype, was significantly less in TLR9$^{-/-}$ mice (Fig. 7A). In contrast, the mRNA expression level of M2 markers FIZZ-1 and Arginase-1 were significantly increased in TLR9$^{-/-}$ mice compared with WT mice (Fig. 7B and C). These data support the functionality of the Th2 cytokine expression profile, which predominates in the TLR9$^{-/-}$ mice even when challenged with antigen known to induce a classic IFN-γ response.

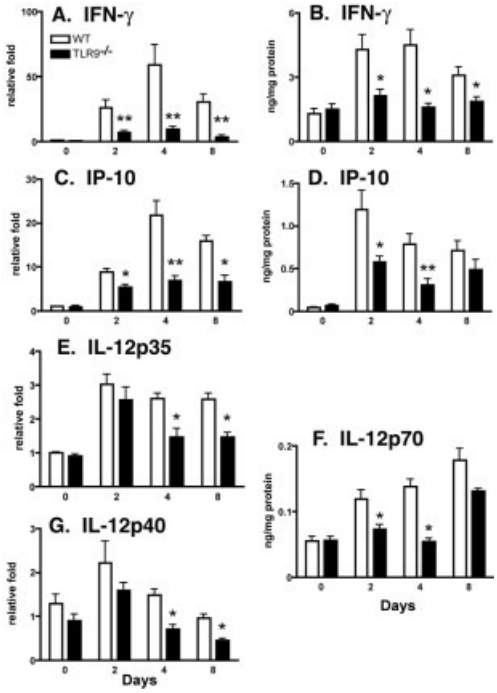

Figure 4. TLR9$^{-/-}$ mice show impaired Th1 chemokine and cytokine levels both in transcript expression and in protein production. On days 0, 2, 4, and 8, total RNA was isolated and reverse transcribed to cDNA. Quantitative real-time PCR (Taqman) was performed to measure the transcript levels of each cytokine. The transcript expression of Th1 cytokines and chemokines, IFN-γ (A), IP-10 (C), IL-12p35 (E), and IL-12p40 (G), was measured. The protein level of IFN-γ (B), IP-10 (D), and IL-12p70 (F) was determined in the whole lungs from mice of WT and TLR9-deficient group by ELISA. The cytokine and chemokine levels in each whole-lung sample were normalized to total protein levels measured using the Bradford assay. Bars are mean ± SD for four to six individual lungs per point. Data are combined studies of three independent experiments. $^*p<0.05$, $^{**}p<0.01$ compared with WT.

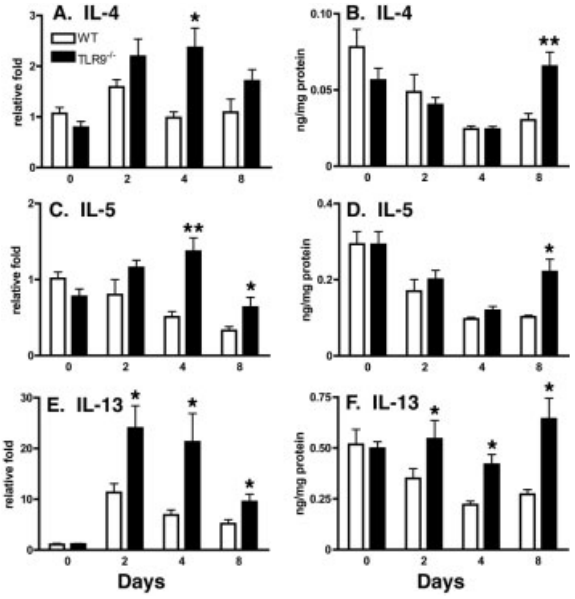

Figure 5. TLR9$^{-/-}$ mice exhibit enhanced Th2 cytokine level both in transcript expression and in protein production. The gene expression level of IL-4 (A), IL-5 (C), and IL-13 (E) in the whole lungs at days 0, 2, 4, and 8 after PPD-bead challenge is shown. mRNA levels were quantitated as described (*Materials and methods* and Fig. 4 legend). The protein level of IL-4 (B), IL-5 (D), and IL-13 (F) was determined in the whole lungs from mice of WT and TLR9-deficient group by ELISA as described (*Materials and methods* and Fig. 4 legend). Bars are mean ± SD for four to six individual lungs per point. Data are combined studies of three independent experiments. $^*p<0.03$, $^{**}p<0.01$ compared with WT.

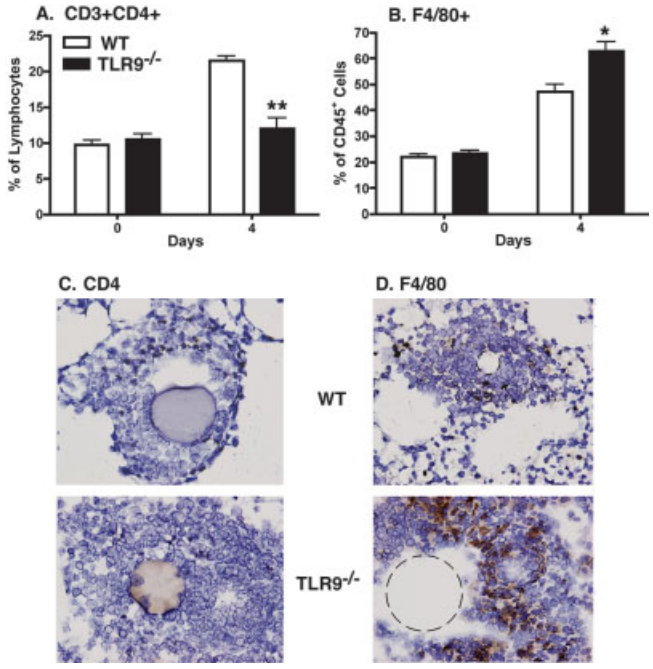

Figure 6. The recruitment of impaired $CD4^+$ T cells and enhanced $F4/80^+$ macrophages during pulmonary granuloma formation in $TLR9^{-/-}$ mice. (A, B) The FACS profiles of lung cells isolated from day 4 PPD-bead challenged mice. Mice killed at day 0 did not receive PPD-beads and were used as baseline values. Lungs were digested by collagenase IV, and the dispersed cells were stained as follows: $CD3^+CD4^+$ (A) and $F4/80^+$ (B). The results shown are representative of two experiments and are expressed as mean ± SEM; n=4–5 lung samples per group out of two independent experiments. $^*p<0.02$, and $^{**}p<0.01$. (C, D) Immunohisitochemical examination of pulmonary granuloma showed fewer $CD4^+$ cells and increased $F4/80^+$ cells in $TLR9^{-/-}$ mice. Dotted lines indicate the area where PPD-beads existed before being washed out by immunohistochemical staining procedure. Cryostat sections were obtained from day 4 bead-challenged lungs and stained for CD4 (C) and F4/80 (D) as described in *Materials and Methods* (magnification, ×400).

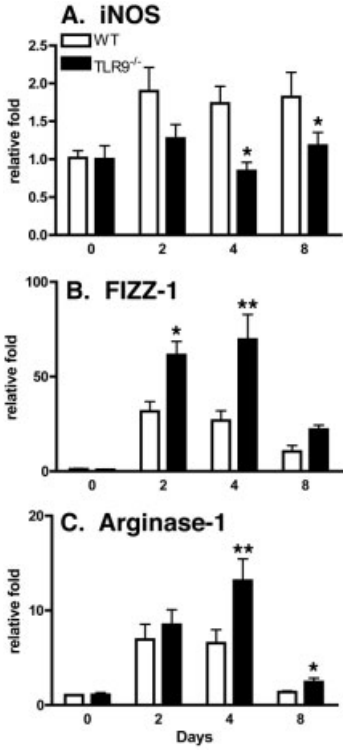

Figure 7. Decreased M1 markers and increased M2 markers during PPD-bead challenge in $TLR9^{-/-}$ mice. The gene expression level of iNOS (A), FIZZ-1 (B) and Arginase-1 (C) in the whole lungs at days 0, 2, 4, and 8 after PPD-bead challenge is shown. mRNA levels were quantitated as described (*Materials and methods* and Fig. 4 legend). $TLR9^{-/-}$ mice exhibited lower transcript level of M1 markers (iNOS), but higher level of M2 markers (FIZZ-1 and Arginase-1). Bars are mean ± SD for four to six individual lungs per point. Data are combined studies of three independent experiments. $^*p<0.02$, $^{**}p<0.01$ compared with WT.

Discussion

Our results demonstrate that the TLR9 signaling pathway is essential in the regulation of the Th1 granuloma response to mycobacterial antigens. To our knowledge, the present investigation represents the first analysis of cell-mediated Th1 pulmonary granuloma formation in mice with targeted disruption of the TLR9 gene. Our study demonstrated that TLR9-deficient mice exhibited significantly larger granuloma formation with a higher eosinophil content, suggesting a shift to a Th2-like response. These histological findings in $TLR9^{-/-}$ mice coincided with significantly decreased whole-lung IFN-γ, IP-10 and IL-12 levels and significantly increased whole-lung levels of IL-4, IL-5, and IL-13 during the formation and maintenance of the granuloma responses when compared with WT mice.

Pulmonary granuloma formation is initiated by a number of infectious and non-infectious agents, and previous studies have illustrated the importance of distinct profiles of cytokines and chemokines in defining the type and predicting sequelae of the granulomatous response [7, 8]. Specifically, the embolization of Sepharose beads coated with PPD from *M. tuberculosis* initiates a Thl-type immune response that is characterized by IFN-γ and IL-12 expression [7]. IL-12 is a key cytokine that promotes IFN-γ production and is known to augment Th1 cell-mediated immune reactions [45], while IFN-γ is essential for the elimination of mycobacteria [46, 47]. Our studies showed impaired expression of IFN-γ and IL-12 in $TLR9^{-/-}$ mice, as well as larger Th2-like granulomas when compared to WT mice, suggesting the pivotal role commanded by TLR9 in driving the Th1-mediated immune response to mycobacterial antigen. In studies using IL-12-knockout mice a decrease in the IFN-γ response and an increased susceptibility of mice to mycobacterium challenge was

observed [48–50], supporting our findings that TLR9$^{-/-}$ mice have larger granulomas with decreased levels of IFN-γ and IL-12. Previous studies indicated that in IFN-γ-deficient mice the type 1 granuloma cytokine profile is shifted to a type 2 pattern [51]: this shift was also observed in our model. TLR9 deficiency increased expression of Th2 cytokines IL-4, IL-5, and IL-13 while significantly decreasing the production of IFN-γ. IL-4 operates as the key cytokine driving the type-2 response [52], IL-5 induces the recruitment of eosinophils [53], and IL-13 is a pleiotropic cytokine produced predominantly by CD4$^+$ Th2 cells. IL-13 is an IL-4-related cytokine, and its receptor contains the IL-4 receptor α1-chain signaling component [54]. IL-13 provides regulatory support to Th2 responses [55], and we have previously demonstrated that antibody-mediated IL-13 depletion increased transcript levels of IFN-γ in a model of Th1-mediated mycobacterial antigen-induced pulmonary granuloma formation [6]. During *M. tuberculosis* infection, TLR9 regulates the Th1 response through IFN-γ and IL-12 production [44]. These studies are consistent with our data showing lower Th1 and higher Th2 cytokine levels during pulmonary granuloma formation in TLR9$^{-/-}$ mice. In contrast to our results showing greater granuloma size in our TLR9$^{-/-}$ model, the study of Bafica and colleagues [44] neither assessed alternations in granuloma pathology nor did they perform a detailed analysis of a model of synchronized inflammation.

In the present study we again demonstrate that macrophages play an important role in granuloma formation. *In vitro*, macrophage activation has been operationally defined across two distinct polarization states, defined as either an M1 or M2 phenotype [13, 16]. However, *in vivo* a continuum between these two states more likely exists. Classically activated (M1) macrophages are prototypical immune effector cells that kill intracellular pathogens *via* the production of oxygen and nitrogen radicals [56]. These cells also secrete a series of proinflammatory cytokines, which help to orchestrate and amplify Th1 immune responses [57]. A second population of macrophages or alternatively activated (M2) macrophages arises in response to an environment dominated by Th2 cytokines, IL-4 and/or IL-13, and they are functionally distinct from M1 macrophages. They fail to produce NO, but they upregulate mannose receptor expression [17]. They express several unique markers such as FIZZ-1 and Ym1, which are not found on M1 macrophages [19]. It has been proposed that the *in vivo* induction of FIZZ-1 in macrophages depends on IL-4 [19]. Additionally, arginase production is significantly increased in M2-polarized macrophages. This enzyme blocks iNOS activity by a variety of mechanisms, including competing for the arginase substrate that is required for NO production [58]. We have demonstrated in this study that the lungs of TLR9$^{-/-}$ mice showed decreased iNOS expression and increased expression of FIZZ-1 and Arginase-1; characteristic of M2 skewing. Our data showing larger granuloma formation in TLR9$^{-/-}$ mice are also consistent with previous study showing that increased NO played a protective role during lung inflammation, and inhibition of NO synthesis during PPD-bead granuloma formation resulted in a change in granuloma size and cellular morphology [59, 60]. The investigation described in this manuscript affirmed the key role of TLR9 in determining macrophage phenotype, as a shift from M1 to M2 macrophages occurred in TLR9$^{-/-}$ mice. Relatedly, another study reported that M2 macrophages failed to stimulate efficient T cell proliferation [57]. We showed here that IP-10 (CXCL10), a chemokine that promotes the migration of activated T cells (Th1 lymphocytes) [61], was decreased in TLR9$^{-/-}$ mice. This finding might underlie the impaired recruitment of CD4$^+$ T cells towards granulomas in TLR9$^{-/-}$ mice.

In summary, we present a comprehensive *in vivo* analysis of TLR9 participation, using TLR9$^{-/-}$ mice, in a model of Th1 granuloma formation induced by mycobacteria-associated antigens. Similar to the IFN-γ knockout mouse [51], TLR9 deficiency resulted in decreased Th1 and increased Th2 cytokine profiles during pulmonary granuloma formation, and led to an accelerated granulomatous response characterized by increased eosinophils. This was associated with decreased CD4$^+$ T cells, enhanced macrophage recruitment, and a significant skewing towards an M2 phenotype. This study supports the concept that an impaired type-1 cytokine profile in TLR9-deficient lungs is a major consequence of larger granuloma formation.

Materials and methods

Mice

Mice (BALB/c) lacking the TLR9 gene (TLR9$^{-/-}$) were provided by Theodore J. Standiford, M.D., University of Michigan Medical School. WT control BALB/c mice were purchased from The Jackson Laboratories (Bar Harbor, ME). All mice were maintained under specific pathogen-free conditions and provided with food and water *ad libitum* in the University Laboratory Animal Medicine (ULAM) facility at the University of Michigan Medical School. All animal protocols were approved by ULAM.

Antibodies

Rat mAb specific for mouse CD3 (17A2), CD4 (L3T4), CD16/32 (2.4G2), CD45 (30-F11) was purchased from BD PharMingen (San Diego, CA). Rat Anti-F4/80 (CI: A3–1) mAb was purchased from Serotec (Raleigh, CA).

Sensitization and granuloma induction

Type 1 lung antigen-bead granulomas were generated as follows. Mice were sensitized i.p. with complete Freund's adjuvant (CFA) (Sigma-Aldrich, St. Louis, MO). After 14–16 days, mice were challenged i.v. with 5500 Sepharose 4B beads (in 0.5 mL PBS) covalently coupled to PPD, as previously described [5]. Mice were killed 2, 4, or 8 days after i.v. injection. This model results in a well-circumscribed lung granuloma typified by a type 1 cytokine phenotype.

Morphometry

Individual excised lung lobes were inflated and fixed with 10% buffered formalin for morphometric analysis. The areas of the granulomas were measured in a blinded fashion on H&E-stained sections of paraffin-embedded lungs using computer-assisted morphometry as previously described [62]. Eosinophil recruitment to the lung granuloma was quantitated and normalized to the granuloma size. A minimum of 20 granulomas per lung section was analyzed for granuloma size, and 20 granulomas per mouse were analyzed for the eosinophil infiltrate [62].

Reverse transcription and real-time quantitative PCR analysis

Total RNA was isolated from whole lungs using TRIzol (Invitrogen Corporation, Carlsbad, CA) according to manufacturer's instructions. Briefly, 2.0 μg RNA was reverse transcribed to yield cDNA in a 25-μL reaction mixture containing 1× first strand (Life Technologies, Gaithersburg, MD), 250 ng oligo(dT) primer, 1.6 mmol/L dNTPs (Invitrogen), 5 U RNase inhibitor (Invitrogen), and 100 U Moloney murine leukemia virus reverse transcriptase (Invitrogen) at 38°C for 60 min; and the reaction was stopped by incubating the cDNA at 94°C for 10 min. Real-time quantitative PCR analysis was performed using an ABI 7700 sequence detector system (PE Applied Biosystems, Foster City, CA). The thermal cycling conditions included 50°C for 2 min and 95°C for 10 min, followed by 40 cycles of amplification at 95°C for 15 s and 55°C for 1.5 min for denaturing and annealing, respectively.

ELISA analysis of chemokine and cytokine expression

Murine IP-10, IL-4, IL-5, IL-12, IL-13, and IFN-γ levels were measured in 50 μL samples from whole lung homogenates using a standardized sandwich ELISA technique previously described in detail [63]. The limit of detection for all ELISA was approximately 50 pg/mL. The chemokine and cytokine levels in each sample were normalized to the protein (in milligrams) present in cell-free preparation of each sample measured by the Bradford assay, as described previously [62].

Flow cytometry

Flow cytometric analyses of lung cells were performed as previously described [62]. Briefly, whole lungs were dispersed in 0.2% collagenase (Sigma-Aldrich) in RPMI 1640 (Mediateck Inc., Herndon, VA) and 5% FBS (Atlas, Fort Collins, CO) at 37°C for 45 min. The cells were stained with FITC-conjugated anti-CD4 mAb and PE-conjugated anti-CD3 mAb for 15 min. $CD3^+CD4^+$ T cells were determined by flow cytometry after gating lymphocyte populations by forward and scatter parameters. In some experiments, cells were stained with PE-conjugated anti-F4/80. The percentage of macrophages was determined as percentage of $CD45^+F4/80^+$ lung cells.

Immunohistochemistry

Mice were killed 4 days after i.v. injection of Sepharose 4B beads covalently coupled to PPD. Acetone-fixed 7-μm cryostat sections were incubated with purified rat mAb specific for mouse anti-CD4 or anti-F4/80 with detection using a Cell and Tissue Staining kit (R&D Systems, Minneapolis, MN) according to manufacture's instructions, followed by color development with HRP-DAB System (R&D Systems).

Statistical analysis

Statistical analysis was performed using Student's *t*-test. The 95% confidence limit was determined significant.

Acknowledgements: This work was supported by NIH (National Institutes of Health) grants HL031963, HL074024, and HL031237. We also thank Robin Kunkel, Valerie Stolberg, Pam Lincoln, and Holly Evanoff for their technical assistance, as well as Dr. Judith Connett for critical reading of the manuscript.

References

1 **Boros, D. L.,** Granulomatous inflammations. *Prog. Allergy* 1978. **24:** 183–267.

2 **El-Zammar, O. A. and Katzenstein, A. L.,** Pathological diagnosis of granulomatous lung disease: a review. *Histopathology* 2007. **50:** 289–310.

3 **Dye, C., Williams, B. G., Espinal, M. A. and Raviglione, M. C.,** Erasing the world's slow stain: strategies to beat multidrug-resistant tuberculosis. *Science* 2002. **295:** 2042–2046.

4 **Ulrichs, T. and Kaufmann, S. H.,** New insights into the function of granulomas in human tuberculosis. *J. Pathol.* 2006. **208:** 261–269.

5 **Chensue, S. W., Ruth, J. H., Warmington, K., Lincoln, P. and Kunkel, S. L.,** *In vivo* regulation of macrophage IL-12 production during type 1 and type 2 cytokine-mediated granuloma formation. *J. Immunol.* 1995. **155:** 3546–3551.

6 **Ruth, J. H., Warmington, K. S., Shang, X., Lincoln, P., Evanoff, H., Kunkel, S. L. and Chensue, S. W.,** Interleukin 4 and 13 participation in mycobacterial (type-1) and schistosomal (type-2) antigen-elicited pulmonary granuloma formation: multiparameter analysis of cellular recruitment, chemokine expression and cytokine networks. *Cytokine* 2000. **12:** 432–444.

7 **Qiu, B., Frait, K. A., Reich, F., Komuniecki, E. and Chensue, S. W.,** Chemokine expression dynamics in mycobacterial (type-1) and schistosomal (type-2) antigen-elicited pulmonary granuloma formation. *Am. J. Pathol.* 2001. **158:** 1503–1515.

8 **Chiu, B. C., Freeman, C. M., Stolberg, V. R., Komuniecki, E., Lincoln, P. M., Kunkel, S. L. and Chensue, S. W.,** Cytokine-chemokine networks in experimental mycobacterial and schistosomal pulmonary granuloma formation. *Am. J. Respir. Cell Mol. Biol.* 2003. **29:** 106–116.

9 **Chiu, B. C., Freeman, C. M., Stolberg, V. R., Hu, J. S., Komuniecki, E. and Chensue, S. W.,** The innate pulmonary granuloma: characterization and

demonstration of dendritic cell recruitment and function. *Am. J. Pathol.* 2004. **164:** 1021–1030.

10 **Chensue, S. W., Warmington, K., Ruth, J., Lincoln, P., Kuo, M. C. and Kunkel, S. L.,** Cytokine responses during mycobacterial and schistosomal antigen-induced pulmonary granuloma formation. Production of Th1 and Th2 cytokines and relative contribution of tumor necrosis factor. *Am. J. Pathol.* 1994. **145:** 1105–1113.

11 **Chensue, S. W., Warmington, K. S., Ruth, J. H., Lincoln, P. and Kunkel, S. L.,** Cytokine function during mycobacterial and schistosomal antigen-induced pulmonary granuloma formation. Local and regional participation of IFN-gamma, IL-10, and TNF. *J. Immunol.* 1995. **154:** 5969–5976.

12 **Gordon, S. and Taylor, P. R.,** Monocyte and macrophage heterogeneity. *Nat. Rev. Immunol.* 2005. **5:** 953–964.

13 **Mantovani, A., Sica, A. and Locati, M.,** New vistas on macrophage differentiation and activation. *Eur. J. Immunol.* 2007. **37:** 14–16.

14 **Goerdt, S. and Orfanos, C. E.,** Other functions, other genes: alternative activation of antigen-presenting cells. *Immunity* 1999. **10:** 137–142.

15 **Lumeng, C. N., Bodzin, J. L. and Saltiel, A. R.,** Obesity induces a phenotypic switch in adipose tissue macrophage polarization. *J. Clin. Invest.* 2007. **117:** 175–184.

16 **Gordon, S.,** Alternative activation of macrophages. *Nat. Rev. Immunol.* 2003. **3:** 23–35.

17 **Stein, M., Keshav, S., Harris, N. and Gordon, S.,** Interleukin 4 potently enhances murine macrophage mannose receptor activity: a marker of alternative immunologic macrophage activation. *J. Exp. Med.* 1992. **176:** 287–292.

18 **Munder, M., Eichmann, K., Moran, J. M., Centeno, F., Soler, G. and Modolell, M.,** Th1/Th2-regulated expression of arginase isoforms in murine macrophages and dendritic cells. *J. Immunol.* 1999. **163:** 3771–3777.

19 **Raes, G., De Baetselier, P., Noel, W., Beschin, A., Brombacher, F. and Hassanzadeh Gh, G.,** Differential expression of FIZZ1 and Ym1 in alternatively *versus* classically activated macrophages. *J. Leukoc. Biol.* 2002. **71:** 597–602.

20 **Herbert, D. R., Holscher, C., Mohrs, M., Arendse, B., Schwegmann, A., Radwanska, M., Leeto, M. *et al.*,** Alternative macrophage activation is essential for survival during schistosomiasis and downmodulates T helper 1 responses and immunopathology. *Immunity* 2004. **20:** 623–635.

21 **Akira, S., Uematsu, S. and Takeuchi, O.,** Pathogen recognition and innate immunity. *Cell* 2006. **124:** 783–801.

22 **Akira, S.,** Mammalian Toll-like receptors. *Curr. Opin. Immunol.* 2003. **15:** 5–11.

23 **Trinchieri, G. and Sher, A.,** Cooperation of Toll-like receptor signals in innate immune defence. *Nat. Rev. Immunol.* 2007. **7:** 179–190.

24 **Uematsu, S. and Akira, S.,** Toll-like receptors and type I interferons. *J. Biol. Chem.* 2007. **282:** 15319–15323.

25 **Krutzik, S. R. and Modlin, R. L.,** The role of Toll-like receptors in combating mycobacteria. *Semin. Immunol.* 2004. **16:** 35–41.

26 **Ryffel, B., Fremond, C., Jacobs, M., Parida, S., Botha, T., Schnyder, B. and Quesniaux, V.,** Innate immunity to mycobacterial infection in mice: critical role for toll-like receptors. *Tuberculosis (Edinb)* 2005. **85:** 395–405.

27 **Jo, E. K., Yang, C. S., Choi, C. H. and Harding, C. V.,** Intracellular signalling cascades regulating innate immune responses to Mycobacteria: branching out from Toll-like receptors. *Cell. Microbiol.* 2007. **9:** 1087–1098.

28 **O'Neill L, A. and Bowie, A. G.,** The family of five: TIR-domain-containing adaptors in Toll-like receptor signalling. *Nat. Rev. Immunol.* 2007. **7:** 353–364.

29 **Kawai, T. and Akira, S.,** TLR signaling. *Semin. Immunol.* 2007. **19:** 24–32.

30 **Scanga, C. A., Bafica, A., Feng, C. G., Cheever, A. W., Hieny, S. and Sher, A.,** MyD88-deficient mice display a profound loss in resistance to Mycobacterium tuberculosis associated with partially impaired Th1 cytokine and nitric oxide synthase 2 expression. *Infect. Immun.* 2004. **72:** 2400–2404.

31 **Fremond, C. M., Yeremeev, V., Nicolle, D. M., Jacobs, M., Quesniaux, V. F. and Ryffel, B.,** Fatal *Mycobacterium tuberculosis* infection despite adaptive immune response in the absence of MyD88. *J. Clin. Invest.* 2004. **114:** 1790–1799.

32 **Reiling, N., Holscher, C., Fehrenbach, A., Kroger, S., Kirschning, C. J., Goyert, S. and Ehlers, S.,** Cutting edge: Toll-like receptor (TLR)2- and TLR4-mediated pathogen recognition in resistance to airborne infection with *Mycobacterium tuberculosis*. *J. Immunol.* 2002. **169:** 3480–3484.

33 **Abel, B., Thieblemont, N., Quesniaux, V. J., Brown, N., Mpagi, J., Miyake, K., Bihl, F. and Ryffel, B.,** Toll-like receptor 4 expression is required to control chronic *Mycobacterium tuberculosis* infection in mice. *J. Immunol.* 2002. **169:** 3155–3162.

34 **Heldwein, K. A., Liang, M. D., Andresen, T. K., Thomas, K. E., Marty, A. M., Cuesta, N., Vogel, S. N. and Fenton, M. J.,** TLR2 and TLR4 serve distinct roles in the host immune response against *Mycobacterium bovis* BCG. *J. Leukoc. Biol.* 2003. **74:** 277–286.

35 **Sugawara, I., Yamada, H., Li, C., Mizuno, S., Takeuchi, O. and Akira, S.,** Mycobacterial infection in TLR2 and TLR6 knockout mice. *Microbiol. Immunol.* 2003. **47:** 327–336.

36 **Drennan, M. B., Nicolle, D., Quesniaux, V. J., Jacobs, M., Allie, N., Mpagi, J., Fremond, C. *et al.*,** Toll-like receptor 2-deficient mice succumb to *Mycobacterium tuberculosis* infection. *Am. J. Pathol.* 2004. **164:** 49–57.

37 **Nicolle, D., Fremond, C., Pichon, X., Bouchot, A., Maillet, I., Ryffel, B. and Quesniaux, V. J.,** Long-term control of *Mycobacterium bovis* BCG infection in the absence of Toll-like receptors (TLRs): investigation of TLR2-, TLR6-, or TLR2-TLR4-deficient mice. *Infect. Immun.* 2004. **72:** 6994–7004.

38 **Hemmi, H., Takeuchi, O., Kawai, T., Kaisho, T., Sato, S., Sanjo, H., Matsumoto, M. *et al.*,** A Toll-like receptor recognizes bacterial DNA. *Nature* 2000. **408:** 740–745.

39 **Jakob, T., Walker, P. S., Krieg, A. M., Udey, M. C. and Vogel, J. C.,** Activation of cutaneous dendritic cells by CpG-containing oligodeoxynucleotides: a role for dendritic cells in the augmentation of Th1 responses by immunostimulatory DNA. *J. Immunol.* 1998. **161:** 3042–3049.

40 **Sparwasser, T., Koch, E. S., Vabulas, R. M., Heeg, K., Lipford, G. B., Ellwart, J. W. and Wagner, H.,** Bacterial DNA and immunostimulatory CpG oligonucleotides trigger maturation and activation of murine dendritic cells. *Eur. J. Immunol.* 1998. **28:** 2045–2054.

41 **Suzuki, Y., Wakita, D., Chamoto, K., Narita, Y., Tsuji, T., Takeshima, T., Gyobu, H. *et al.*,** Liposome-encapsulated CpG oligodeoxynucleotides as a potent adjuvant for inducing type 1 innate immunity. *Cancer Res.* 2004. **64:** 8754–8760.

42 **Huang, L. Y., Ishii, K. J., Akira, S., Aliberti, J. and Golding, B.,** Th1-like cytokine induction by heat-killed *Brucella abortus* is dependent on triggering of TLR9. *J. Immunol.* 2005. **175:** 3964–3970.

43 **Edwards, L., Williams, A. E., Krieg, A. M., Rae, A. J., Snelgrove, R. J. and Hussell, T.,** Stimulation *via* Toll-like receptor 9 reduces *Cryptococcus neoformans*-induced pulmonary inflammation in an IL-12-dependent manner. *Eur. J. Immunol.* 2005. **35:** 273–281.

44 **Bafica, A., Scanga, C. A., Feng, C. G., Leifer, C., Cheever, A. and Sher, A.,** TLR9 regulates Th1 responses and cooperates with TLR2 in mediating optimal resistance to *Mycobacterium tuberculosis*. *J. Exp. Med.* 2005. **202:** 1715–1724.

45 **Kennedy, M. K., Picha, K. S., Shanebeck, K. D., Anderson, D. M. and Grabstein, K. H.,** Interleukin-12 regulates the proliferation of Th1, but not Th2 or Th0, clones. *Eur. J. Immunol.* 1994. **24:** 2271–2278.

46 **Flynn, J. L., Chan, J., Triebold, K. J., Dalton, D. K., Stewart, T. A. and Bloom, B. R.,** An essential role for interferon gamma in resistance to *Mycobacterium tuberculosis* infection. *J. Exp. Med.* 1993. **178:** 2249–2254.

47 **Jouanguy, E., Doffinger, R., Dupuis, S., Pallier, A., Altare, F. and Casanova, J. L.,** IL-12 and IFN-gamma in host defense against mycobacteria and salmonella in mice and men. *Curr. Opin. Immunol.* 1999. **11:** 346–351.

48 **Cooper, A. M., Kipnis, A., Turner, J., Magram, J., Ferrante, J. and Orme, I. M.,** Mice lacking bioactive IL-12 can generate protective, antigen-specific cellular responses to mycobacterial infection only if the IL-12 p40 subunit is present. *J. Immunol.* 2002. **168:** 1322–1327.

49 **Cooper, A. M., Magram, J., Ferrante, J. and Orme, I. M.,** Interleukin 12 (IL-12) is crucial to the development of protective immunity in mice intravenously infected with *Mycobacterium tuberculosis*. *J. Exp. Med.* 1997. **186:** 39–45.

50 **Holscher, C., Atkinson, R. A., Arendse, B., Brown, N., Myburgh, E., Alber, G. and Brombacher, F.,** A protective and agonistic function of IL-12p40 in mycobacterial infection. *J. Immunol.* 2001. **167:** 6957–6966.

51 **Chensue, S. W., Warmington, K., Ruth, J. H., Lukacs, N. and Kunkel, S. L.,** Mycobacterial and schistosomal antigen-elicited granuloma formation in IFN-gamma and IL-4 knockout mice: analysis of local and regional cytokine and chemokine networks. *J. Immunol.* 1997. **159:** 3565–3573.

52 **Cheever, A. W. and Yap, G. S.,** Immunologic basis of disease and disease regulation in schistosomiasis. *Chem. Immunol.* 1997. **66:** 159–176.

53 **Sehmi, R., Wardlaw, A. J., Cromwell, O., Kurihara, K., Waltmann, P. and Kay, A. B.,** Interleukin-5 selectively enhances the chemotactic response of eosinophils obtained from normal but not eosinophilic subjects. *Blood* 1992. **79:** 2952–2959.

54 **Zurawski, S. M., Chomarat, P., Djossou, O., Bidaud, C., McKenzie, A. N., Miossec, P., Banchereau, J. and Zurawski, G.,** The primary binding subunit of the human interleukin-4 receptor is also a component of the interleukin-13 receptor. *J. Biol. Chem.* 1995. **270:** 13869–13878.

55 **Chiaramonte, M. G., Schopf, L. R., Neben, T. Y., Cheever, A. W., Donaldson, D. D. and Wynn, T. A.,** IL-13 is a key regulatory cytokine for Th2 cell-mediated pulmonary granuloma formation and IgE responses induced by *Schistosoma mansoni* eggs. *J. Immunol.* 1999. **162:** 920–930.

56 **Nathan, C. and Shiloh, M. U.,** Reactive oxygen and nitrogen intermediates in the relationship between mammalian hosts and microbial pathogens. *Proc. Natl. Acad. Sci. USA* 2000. **97:** 8841–8848.

57 **Edwards, J. P., Zhang, X., Frauwirth, K. A. and Mosser, D. M.,** Biochemical and functional characterization of three activated macrophage populations. *J. Leukoc. Biol.* 2006. **80:** 1298–1307.

58 **Munder, M., Eichmann, K. and Modolell, M.,** Alternative metabolic states in murine macrophages reflected by the nitric oxide synthase/arginase balance: competitive regulation by $CD4^+$ T cells correlates with Th1/Th2 phenotype. *J. Immunol.* 1998. **160:** 5347–5354.

59 **Hogaboam, C. M., Chensue, S. W., Steinhauser, M. L., Huffnagle, G. B., Lukacs, N. W., Strieter, R. M. and Kunkel, S. L.,** Alteration of the cytokine phenotype in an experimental lung granuloma model by inhibiting nitric oxide. *J. Immunol.* 1997. **159:** 5585–5593.

60 **Hogaboam, C. M., Gallinat, C. S., Bone-Larson, C., Chensue, S. W., Lukacs, N. W., Strieter, R. M. and Kunkel, S. L.,** Collagen deposition in a non-fibrotic lung granuloma model after nitric oxide inhibition. *Am. J. Pathol.* 1998. **153:** 1861–1872.

61 **Loetscher, M., Gerber, B., Loetscher, P., Jones, S. A., Piali, L., Clark-Lewis, I., Baggiolini, M. and Moser, B.,** Chemokine receptor specific for IP10 and mig: structure, function, and expression in activated T-lymphocytes. *J. Exp. Med.* 1996. **184:** 963–969.

62 **Wen, H., Hogaboam, C. M., Gauldie, J. and Kunkel, S. L.,** Severe sepsis exacerbates cell-mediated immunity in the lung due to an altered dendritic cell cytokine profile. *Am. J. Pathol.* 2006. **168:** 1940–1950.

63 **Evanoff, H. L., Burdick, M. D., Moore, S. A., Kunkel, S. L. and Strieter, R. M.,** A sensitive ELISA for the detection of human monocyte chemoattractant protein-1 (MCP-1). *Immunol. Invest.* 1992. **21:** 39–45.

